A Comparative Study on Ni-Zn-Ga Ferrites Irradiated by Thermal Neutrons

Kh. Roumaih[1*]

[1]*Department of Reactor Physics, Nuclear Research Center, Atomic Energy Authority, Cairo, Egypt.*

Author's contribution

The sole author designed, analysed, interpreted and prepared the manuscript.

Article Information

Original Research Article

ABSTRACT

The chemical formulae $Ni_{1-x}Zn_xGa_{0.5}Fe_{1.5}O_4$ (x= 0, 0.5, and 1) with spinel structure was prepared by a solid-state reaction at 1200 °C. The effect of irradiation by thermal neutrons is discussed on the structure by X-ray diffraction and by the Fourier transforms infrared absorption. After irradiation, the unit cell of the sample NZGF1 is expended, but for the samples NZGF2 and NZGF3 the unit cell is compressed. The cation distribution for all samples has been estimated according to the theoretical lattice parameters before and after irradiated. The spectra of FTIR show two bands, the band $v1$ (611–563 cm^{-1}) shifted to lower whereas the band $v2$ (428–435 cm^{-1}) shifted to increases. The vibrating sample magnetometer (VSM) was measured before and after irradiation. The results of magnetic properties show a decrease in introducing Zn ions and by irradiation. It can be concluded that these compositions are convenient as a radiation detector materials.

1. INTRODUCTION

The general formula of the spinel structure AB_2O_4 is $(A^{2+})[B_2^{3+}]O_4^{2-}$ is face-centred cubic, in which the unit cell is formed by 32 oxygen ions that form 64 tetrahedral cations which is divalent metal ions (A^{2+}), and 32 octahedral cations which is trivalent ions [B^{3+}]. The probability of the

Corresponding author: Email: khroumaih@yahoo.com;

classification of the spinel structure is three types: normal, inverse, and mixed spinel based on the cation occupancy [1,2]. In a normal spinel, the divalent metal ions should be occupied the tetrahedral sites (A) and the trivalent metal ions should be occupied octahedral sites [B]. Examples of such normal spinels include $MgAl_2O_4$, and $ZnFe_2O_4$. In the inverse-spinel structure, the position is inversed i.e. the tetrahedral sites occupied by half of the B cations and the other half will occupy the octahedral, while the all (A) cations occupy the octahedral sites. It is denoted as $(B^{3+})[A^{2+}B^{3+}]\,O_4$. $CoFe_2O_4$ and $NiFe_2O_4$ are examples of the inverse-spinel structure [3,4]. In a mixed spinel, it is mixed between A and B cations occupy both octahedral and tetrahedral sites, and the molecular formula is $(M_x^{2+}Fe_{1-x}^{3+})[M_{1-x}^{2+}Fe_{1+x}^{3+}]O_4$. Examples of mixed spinels include $NiCo_2O_4$, $MnCo_2O_4$, and $CoMn_2O_4$. Generally, the spinel ferrites AB_2O_4 have been good electrical and magneto-optical properties, according to the A- and B-site cation distribution and they possess widely investigated for applications in different fields, including the electronics industry, magnetic recording, magnetic resonance imaging, and ferrofluid [5,6].

There are several studies done [7-11] on the irradiation effects induced by gamma rays on the ferrite, but the study of the irradiation by thermal neutron are very rare. The previous works on $Ni_{1-x}Zn_xGa_yFe_{2-y}O_4$ [7,12-13] do not study the effect of radiation on structure, and the step of x = 0.0, 0.5, and 1 do not study. This work studies the effect of a weak dose of thermal neutron irradiation on the structure and the magnetic properties of $Ni_{1-x}Zn_xGa_{0.5}Fe_{1.5}O_4$ (x= 0, 0.5, and 1). The dose of thermal neutron irradiation was weak because we want to measure the sensitivity of our samples for weak radiation for using as a radiation–detector.

2. MEASUREMENTS AND CALCULATION

2.1 Preparation and Irradiation

The conventional ceramic technique used to prepare the system $Ni_{1-x}Zn_xGa_{0.5}Fe_{1.5}O_4$: where x = 0.0, 0.5, and 1. The starting materials were Nickel oxide (NiO), Zinc oxide (ZnO), Gallium oxide (Ga_2O_3) and ferric oxide α-Fe_2O_3, all materials with high purity 99.99%. The samples were pre-sintered at temperatures 1423 K for 72 h and followed by slow cooling to room temperature. The homogeneous powder was obtained by reground for 2 h and sintered again at temperatures 1473 K for 10 h, and followed by slow cooling to room temperature. The system $Ni_{1-x}Zn_xGa_{0.5}Fe_{1.5}O_4$ with x = 0.0, 0.5 and 1.0, were labeled as NZGF1, NZGF2 and NZGF3, respectively. The prepared samples were irradiated by thermal neutrons using a rabbit system for 2 sec with dose of 2.3 Gy at ET-RR2 Reactor, Nuclear Research Center, Atomic Energy Authority, Egypt. The unirradiated and irradiated process was labelled as Z0 and Z1, respectively.

2.2 Structural Characterization and Calculation

The crystal structure, purity and homogeneity of the prepared samples were checked by X-ray diffraction (XRD) using a XD-D1 X-ray diffractometer with the CuKα radiation (λ = 1.5404 Å), and a nickel filter in the interval 2θ = $10°$–$80°$ at a step scan of $0.02°$ with time 2 s. From X-ray diffraction the lattice constant (a_{XRD}) of the unit cell was calculated using the following equation:

$$a_{XRD} = d\sqrt{(h^2 + k^2 + l^2)} \qquad (1)$$

where, d is the inter-planer spacing in XRD pattern (=2 sin θ /λ) and (hkl) is the Miller indices of the diffraction plane. To compare the lattice constant obtained from the XRD data and the theoretically estimated values, we have calculated the theoretical lattice constant (a_{th}) based on the ionic radii of cations at A and B sites; using the following expression [14]:

$$a_{th} = (8/3\sqrt{3})[(r_A + R_O) + \sqrt{3}\,(r_B + R_O)] \qquad (2)$$

where, r_A and r_B are the cationic radii at A- and B-sites, respectively, and R_O is the oxygen ion radius. The ionic radii of cations are dependent upon their coordination, 4 and 6 oxygen ions are surrounding the tetrahedral (A) and octahedral (B) sites respectively. Here, Ni_A^{+2} (0.55Å), Zn_A^{+2} (0.60Å), Ga_A^{+3} (0.47Å), Fe_A^{+3} (0.49Å), Ni_B^{+2} (0.69Å), Zn_B^{+2} (0.74Å), Ga_B^{+3} (0.62Å), Fe_B^{+3} (0.645Å), and O^{-2} (1.38Å) in cubic close-packed geometry [15]. The radii of ions on tetrahedral and octahedral sites, r_A and r_B respectively are given by [16]:

$$r_A = C_{Fe}r(Fe^{3+}) + C_{Ni}r(Ni^{2+}) + C_{Ga}r(Ga^{3+}) + C_{Zn}r(Zn^{2+}) \qquad (3)$$

$$r_B = \tfrac{1}{2}[C_{Fe}r(Fe^{3+}) + C_{Ni}r(Ni^{2+}) + C_{Ga}r(Ga^{3+}) + C_{Zn}r(Zn^{2+})] \qquad (4)$$

where, $r(Fe^{3+})$, $r(Ni^{2+})$, $r(Ga^{3+})$, and $r(Zn^{2+})$ are the ionic radii of Fe^{3+}, Ni^{2+}, Ga^{3+}, and Zn^{2+} ions. While C_{Fe}, C_{Ni}, C_{Ga}, and C_{Zn} are the concentration of the cation in A- and B- sites, respectively.

The average bond lengths between cations in both A- and B- sites, and oxygen R_A and R_B, respectively, are given by:

$$R_A = r_A + R_o \quad \text{and} \quad R_B = r_B + R_o \tag{5}$$

The oxygen position parameter u can be determined from the relation,

$$r_A = a\sqrt{3}\,(u\text{ -0.25}) - R_O \quad \text{or}$$
$$r_B = a\,(5/8 - u) - R_O \tag{6}$$

To identify the chemical bonds and functional groups of our system, the FTIR spectrum recorded in the wavenumber range of 4000–400 cm^{-1}, using a FTIR spectrometer (Perkin Elmer, Spectrum 100, USA). The spring-model of vibration of atoms is the principle of FTIR spectroscopy, while the wave number ν of vibration is given by [17]:

$$\nu^2 = F/4\pi^2 c^2 M \tag{7}$$

where, F is the spring (force) constant, M is the reduced mass of ions involved and c is the velocity of light. The force constant is reflected of bond strength.

The VSM behavior of the prepared samples was investigated with maximum magnetic field (H) of 20 kOe using LakeShore 7410 at room temperature. The parameters such as the saturation magnetization (M_S) and coercivity (H_C) are calculated from the loops. The magnetic moment per formula unit in Bohr magneton μ_B can be calculated using the following relation [18]:

$$\mu_B = (M_w \times M_s)/5585 \tag{8}$$

where, M_w is the molecular weight of the particular composition, M_s is the saturation magnetization (emu/gm) and the constant 5585 is the magnetic factor. The squareness ratio of all samples are calculated using the relation (S = Mr/Ms).

3. RESULTS AND DISCUSSION

3.1 X-Ray Analysis

Fig. 1(a, and b) shows the XRD patterns for the synthesized samples NZGF1, NZGF2 and NZGF3, before and after irradiation. All patterns are single phase and show the stability of the crystalline structure and no other phases are found after irradiation. The planes (111), (220), (311), (222), (400), (422), (511), and (440) are in good agreement with the cubic spinel structure. It is noticed that, the position of 2θ is slightly shifted to lower angle with introducing the Zn ions, which lead to increase the interplanar distance (d) and increasing the lattice constant (Eq.1) of the unit cell. The lattice parameters (a_{XRD}, a_{th}, R_A, R_B) before and after irradiation samples are presented in Table 1. The tabulated values show that the lattice constant (a_{XRD}) for all samples increases with introducing the Zn ions, due to the ionic radii of Zn ion is large than that substituted by Ni ions. As the results of introducing Zn ions, the bonding length (R_A) is increased i.e. the lattice is expanded. A quantitative measure of the distance between an oxygen ion and cations in unit cell, this displacement is the oxygen positional parameter u= 3/8 = 0.375Å. If any deviation from the perfect value of u= 3/8 = 0.375Å due to the accommodation of relatively large or small ions, distortion of the lattice structure will occur. So, when the parameter u is changed, the unit cell will be distorted. The oxygen positional parameter u for all samples before and after irradiation is calculated in tabulated in Table 1, and notice that, the u parameters are increased i.e. the lattice constant will be increased which indicates expanded of the unit cell as mentioned above. Also, the values of bonding length R_A is increased by introducing Zn^{2+} ion which indicated that, the Zn^{2+} ions will be going to A-site. To ensure the exactness of the proposed distribution, lattice parameters for the NZGF ferrite have been calculated theoretically and summarized in Table 1. From Table 1 the theoretical values are in good approaches with experimental values and they both have the same trend.

In the Ni-Zn ferrite [19], the Zn^{2+} ions have strong preference for A-sites due to their sp3 covalence and the Ni^{2+} ions strong preference for B-sites because of their higher octahedral crystal field stabilization energy (CFSE) equally showed while the Fe^{3+} ions no preference for any of the sites because of have zero CFSE, i.e. the Fe^{3+} ions in both the sites. Also, Ga ions are no preference for any of the sites according to the measurements of Mössbauer Effect [12]. Therefore, according to the calculation of lattice parameters for the sample $NiGa_{0.5}Fe_{1.5}O_4$ the estimated cation distribution before radiation is tabulated in Table 2.
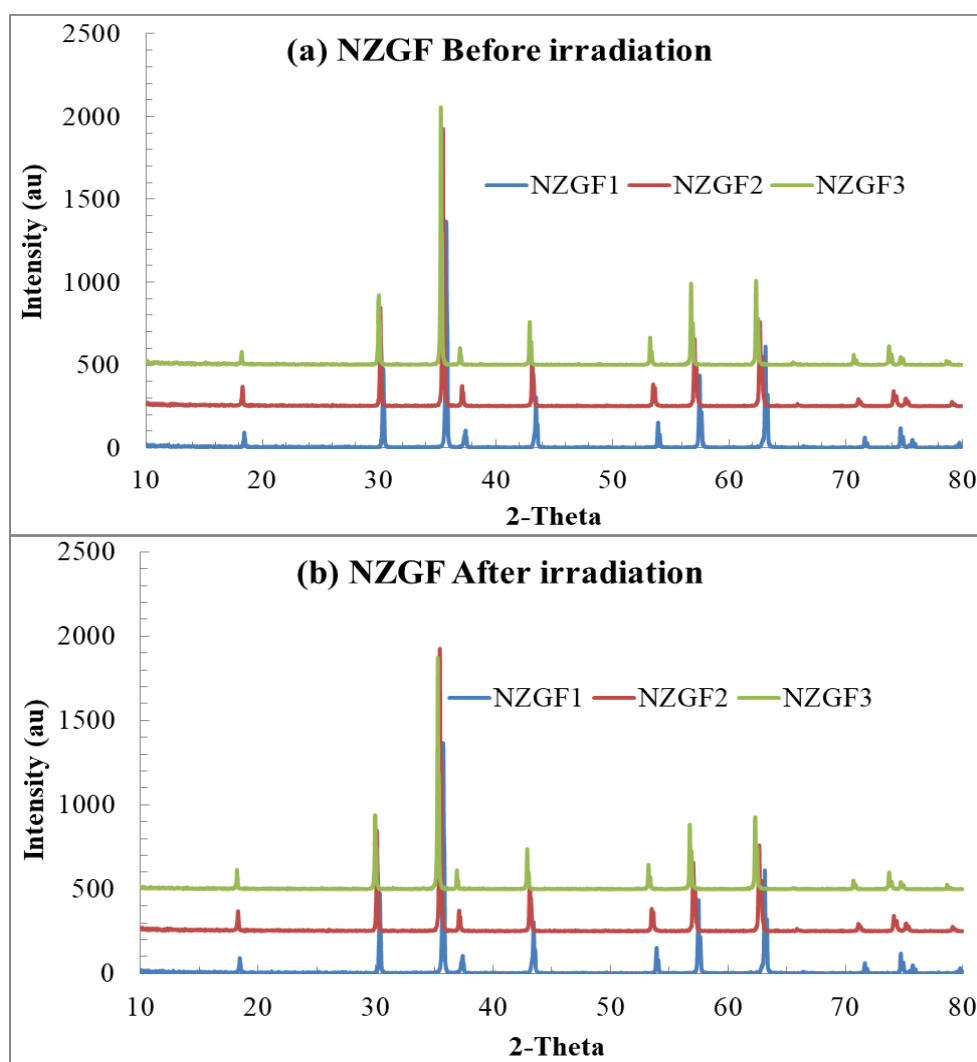
Fig. 1(a-b). The X-ray diffraction patterns of NZGF ferrites before and after irradiation

Table 1. The lattice parameters for $Ni_{1-x}Zn_xGa_{0.5}Fe_{1.5}O_4$ before (Z0) and after (Z1) irradiation

Sample	$a_{(XRD)}$ (Z0)	$a_{(th)}$ (Z0)	R_A (Z0)	R_B (Z0)	u (Å) (Z0)	$a_{(XRD)}$ (Z1)	$a_{(th)}$ (Z1)	R_A (Z1)	R_B (Z1)	u (Å) (Z1)
NZGF1	8.329	8.324	1.860	2.048	0.379	8.375	8.342	1.860	2.054	0.378
NZGF2	8.418	8.377	1.925	2.030	0.382	8.375	8.395	1.925	2.037	0.391
NZGF3	8.420	8.419	1.980	2.019	0.386	8.417	8.450	1.980	2.026	0.386

Table 2. Cation distribution before (Z0) and after (Z1) irradiation

Sample	Before irradiation		After irradiation	
	A-site	B-site	A-site	B-site
NZGF1	$Fe_{0.5}Ga_{0.5}$	Ni_1Fe_1	$Fe^{+3}_{0.5}Ga^{+3}_{0.5}$	$Ni^{+2}_1Fe^{+3}_{0.9}Fe^{+2}_{0.1}$
NZGF2	$Fe_{0.5}Zn_{0.5}$	$Ni_{0.5}Ga_{0.5}Fe_1$	$Fe^{+3}_{0.5}Zn^{+2}_{0.5}$	$Ni^{+2}_{0.5}Ga^{+3}_{0.5}Fe^{+3}_{0.9}Fe^{+2}_{0.1}$
NZGF3	Zn_1	$Ga_{0.5}Fe_{1.5}$	Zn^{+2}_1	$Ga^{+3}_{0.5}Fe^{+3}_{1.4}Fe^{+2}_{0.1}$

The effect of irradiation by thermal neutrons on the unit cell of NZGF, we notice that, the sample NZGF1 after irradiation, the experimental lattice constant (a_{XRD}) is increased i.e. the unit cell is expended, but for the samples NZGF2 and NZGF3 decreased i.e. the unit cell is compressed after irradiation. This distortion may be due to the formation of ferrous ions (Fe^{2+}) with

larger radius (0.76 Å), as reported in many studies [7-9,20-22]. After irradiation, the lattice parameter of NZGF samples not only depend on Zn^{2+} content but also depend on the distorted lattice formed by thermal neutron irradiation. The estimated cation distribution after irradiation by thermal neutrons is tabulated in Table 2. The number of ferrous ions must be adjusted to reach the best matching between theoretical and experimental structures and magnetic parameters.

3.2 FT-IR Analysis

FT-IR spectra for the system NZGF ferrite before and after irradiation in the frequency range 4000–400 cm^{-1} are shown in Fig. 2(a, b, and c). The information of the chemical and molecular structure changes in the ferrite will be known by infrared spectroscopy according to the changes in the Fe^{3+}-O^{2+} bond when some foreign atom is introduced in the parent ferrite compound and/or during heat treatment or after irradiation. According to Waldron [23] the ferrites have two distinct bands in the range 1000-300 cm-1 corresponding to the tetrahedral (A-) and the octahedral (B-) site, represented as *v1* and *v2*, respectively. The band *v1* and the band *v2* were obtained from the stretching vibration of the unit cell in the A-site, and the metal-oxygen vibration in the B-site, respectively [24]. Otherwise, this range will be for the free or absorbed water H-O-H 1000-1200 cm^{-1}, the carboxylate groups (COO− stretching) 1400-1600 cm^{-1} and the hydrocarbon chain (CH2 and CH3 groups) 2800-3000 cm^{-1}. As seen in Fig. 2 (a, b) show two main absorption bands: *v1* (611–563 cm^{-1}) shifts to lower wave numbers whereas *v2* (428–435 cm^{-1}) shifts to increases with introducing Zn ions. The vibrational frequencies of the IR bands corresponding to tetrahedral and octahedral sites (before and after irradiation) are given in Table 3. Generally, the values of the vibration frequencies change with changing the bond length in the spinel unit cell as a result of substituting elements with different ionic radii [25]. So, the introduce of Zn^{2+} ions which has larger radius and greater atomic weight will increase the bond length (R_A) as maintained in XRD which reflects to decrease the (*v1*) in the tetrahedral site. On the other hand, the migration of Fe^{3+} ions to the B-site with a comparatively smaller radius and low atomic weight will decrease the bond length (R_B) which reflects to increase the frequency of vibration in the octahedral site (*v2*). The above discussions are reflected well for unirradiated and irradiated samples.

The force constants corresponding to the tetrahedral F_T and octahedral F_O sites, calculated by using:

$$F_T = 7.62 \times M1 \times v_1^2 \times 10^{-7} \tag{9}$$

$$F_O = 10.62 \times (M2/2) \times v_2^2 \times 10^{-7} \tag{10}$$

where M1 and M2 are the molecular weight of tetrahedral and octahedral sites, respectively. The values of force constant for tetrahedral (F_T) and octahedral (F_O) sites are listed in Table 3. This table shows that, the force constant of A-site (F_T) is found to be higher than that of the B-site (F_O). This can be due to the stronger interaction between cations and oxygen ions at A-site than that B-site [26]. This explains why the bond length R_A is shorter than the bond length R_B (Table 1). In other words, the increasing in bond length should lead to a decrease in force constant.

Generally, in case of inverse and/or mixed spinel ferrites, the variation of the bond strengths between the same cation present in both sites (such as Fe) and their strong interaction with each other, broadens and in some cases splits of bands [17]. Fig. 2c shows clear broadens and split of the sample NZGF3 due to irradiation by thermal neutrons. It is noticed that the broadness of octahedral band (*v2*) is less than the tetrahedral band (*v1*). This indicates the cations at the octahedral sites have a high stability than the cations at the tetrahedral site after irradiation by thermal neutrons. In another word, the effect of irradiation by thermal neutrons on the samples which contain Zn ions will increase the interaction cations at both sites (tetrahedral and octahedral), and increases the constant force and frequency band. Therefore, ferric ions exposed to thermal neutrons are changed to ferrous ions this tends to broad and shift of the absorbed bands. The obtained evidence in our composition explains the distortion of the lattice after irradiation which indicates the useful properties of this composition for detecting nuclear pollution.

3.3 VSM Analysis

Fig. 3 (a-c) shows the hysteresis curves versus magnetic field for the NZGF ferrite system before and after irradiation measured by VSM with the maximum applied the field of ±20 kOe. Table 4 summarizes the magnetization parameters (M_S, M_r, H_C, $\mu_{(exp)}$, and $\mu_{(th)}$). These values show that the magnetization parameters have decreased

by introducing the Zn ions. This due to, the magnetic moment of Zn^{2+} and Ga^{+3} (0 μ_B), but for Ni^{+2} is (2.9 μ_B), and for Fe^{3+} is (5 μ_B). As mentioned above, the interaction cations at both sites (tetrahedral and octahedral) increased due to the irradiation by thermal neutrons which reflects the magnetic properties of the samples. Therefore, the saturation magnetization (M_S) decreases with the increasing of Zn^{2+} ions 66 - 1.8968e mu/g. The values of saturation magnetization for NZGF1 is high decreased by irradiation, due to the formation of ferrous (Fe^{2+}) ions in B-site which have magnetic moment (4 μ_B) less than ferric ions (Fe^{3+}) (5 µB). As seen in Fig. 3, the loops have a small

coercivity H_C, which indicate a soft magnetic behaviour of the samples under investigation. From table it is clear that the squareness ratio ($S=Mr/Ms$) is found to be very low <0.5 for all samples, which indicate the formation of multi-domain grains.

From the estimated cation distribution of NZGF samples, it was necessary to calculate the theoretical magnetic net moment u_{th} to verify the cation distribution of our samples before and after irradiation. According to Neel's model of ferrimagnetism which have two sub-lattice [27], the net moment per formula is given by $u_{th} = M_B(x) − M_A(x)$, where M_A and M_B are the
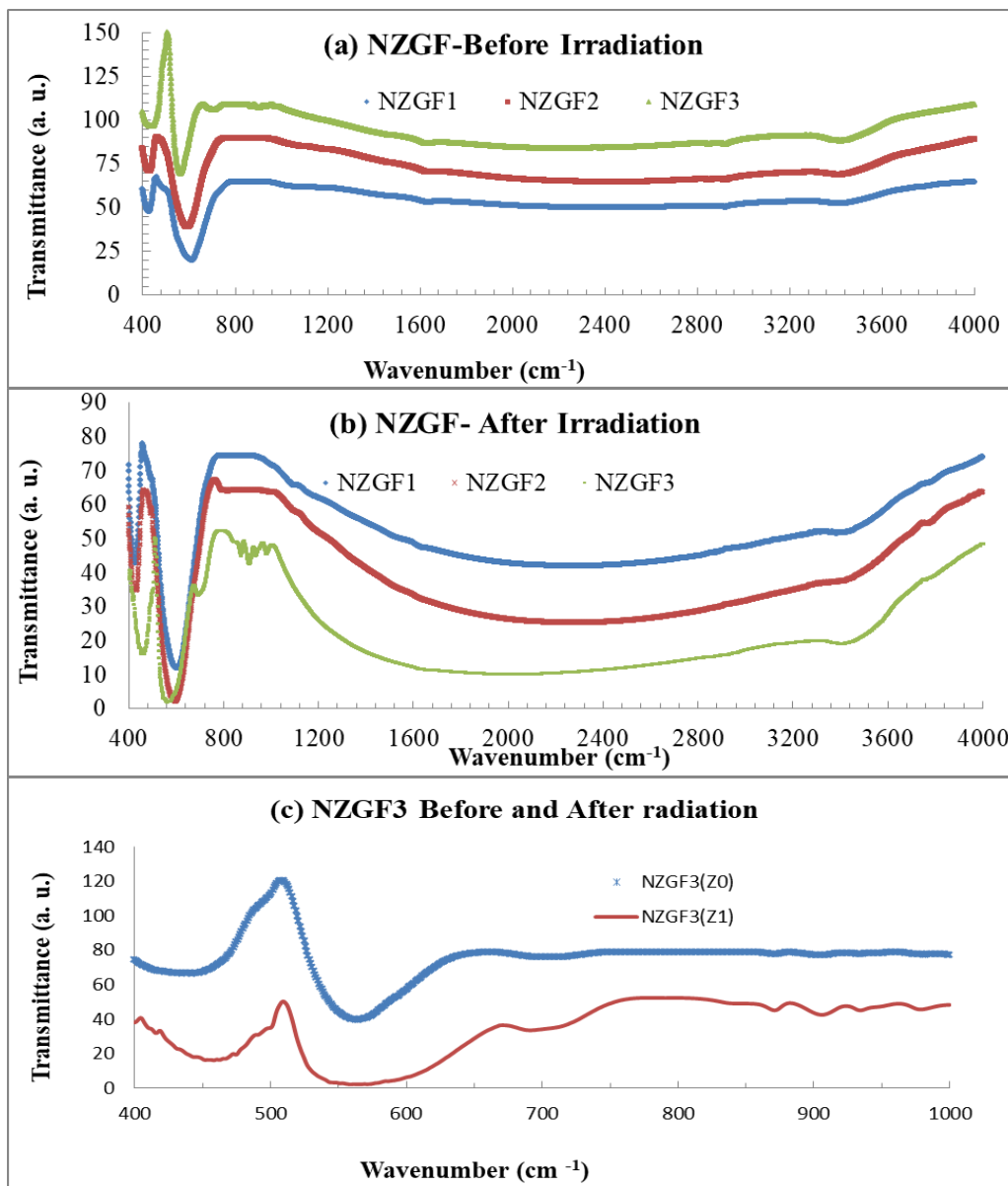

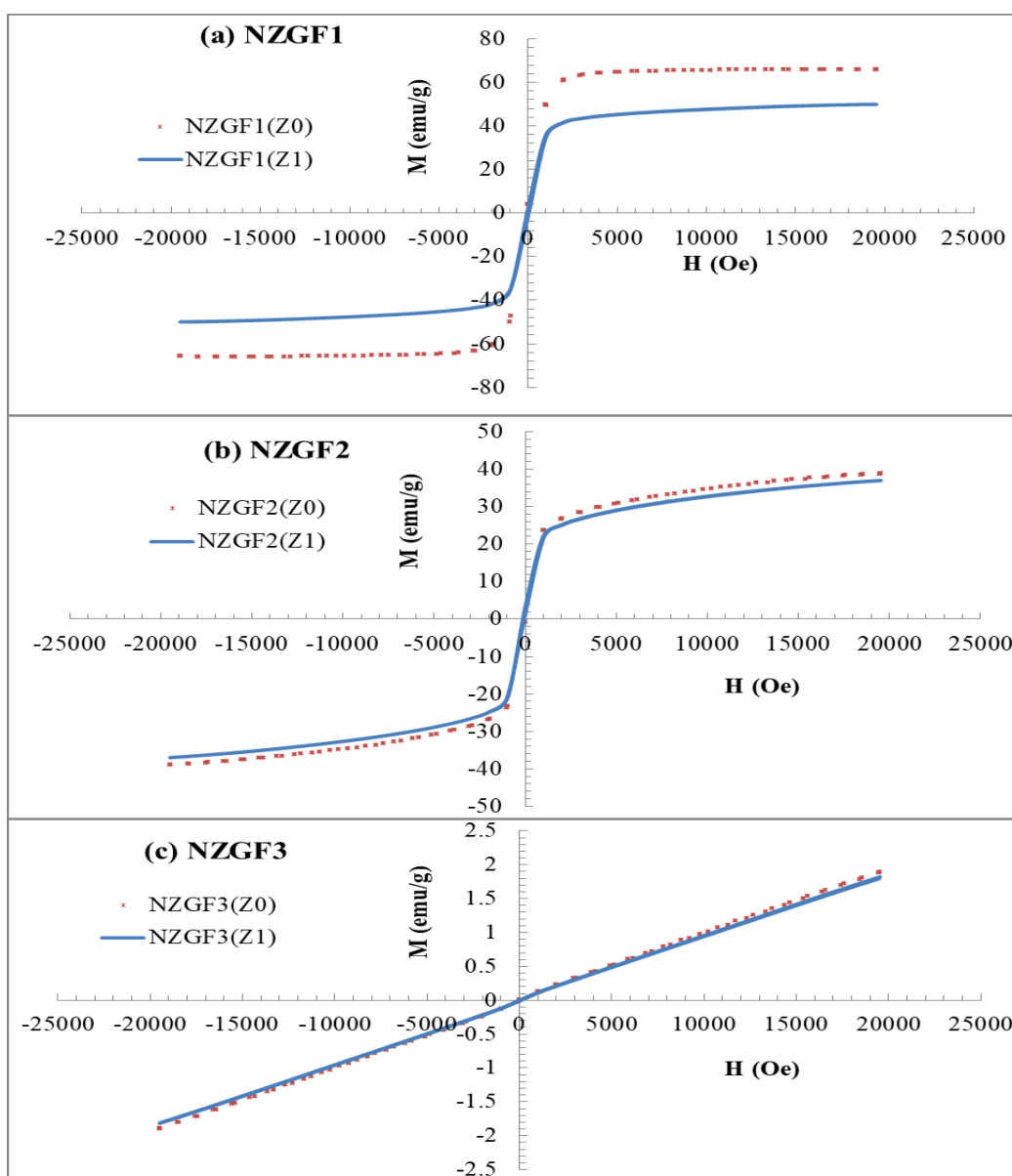**Fig. 2(a-c). The FTIR spectra of NZGF ferrites before and after irradiation**

Fig. 3. The VSM spectra of NZGF ferrites before and after irradiation

Table 3. FTIR absorption band position (ν1, and ν2), and force constants (F_T, and F_O) of Ni$_{1-x}$Zn$_x$Ga$_{0.5}$Fe$_{1.5}$O$_4$ before (Z0) and after (Z1) irradiation

Sample	ν1 cm^{-1} (Z0)	ν2 cm^{-1} (Z0)	F_T N/m (Z0)	F_O N/m (Z0)	ν1 cm^{-1} (Z1)	ν2 cm^{-1} (Z1)	F_T N/m (Z1)	F_O N/m (Z1)
NZGF1	611	427	17.86	11.09	603	428	17.40	11.14
NZGF2	595	430	16.35	11.79	599	435	16.57	12.063
NZGF3	563	435	15.10	12.20	566	458	15.26	13.53

A and B sub-lattice magnetic moments in μ_B. Neel's magnetic moment has been calculated for samples NZGF1 and NZGF2, but NZGF3 sample has not the interaction between sub-lattice. The experimental magnetic moment $\mu_{(exp)}$ is calculated per formula and tabulated with theoretical magnetic net moment u_{th} in Table 4. They both have the same trend and it confirms the estimated cation distributions for NZGF samples.

Table 4. Magnetic parameters for $Ni_{1-x}Zn_xGa_{0.5}Fe_{1.5}O_4$ before (Z0) and after (Z1) irradiation

Sample	M_S (emu/g) Z0	M_r (emu/g) Z0	H_C (Oe) Z0	$\mu_{(ex)}$ Z0	$\mu_{(th)}$ Z0	M_S (emu/g) Z1	M_r (emu/g) Z1	H_C (Oe) Z1	$\mu_{(ex)}$ Z1	$\mu_{(th)}$ Z1
NZGF1	65.985	2.284	44.945	2.85	5.4	49.959	1.542	42.145	2.16	4.6
NZGF2	38.948	0.909	36.857	1.71	3.95	37.009	0.667	26.701	1.62	3.6
NZGF3	1.8968	0.005	40.174	0.08	-	1.8191	0.004	35.426	0.08	-

4. CONCLUSIONS

The objective of this study to measure the sensitivity of $Ni_{1-x}Zn_xGa_{0.5}Fe_{1.5}O_4$ (x= 0, 0.5, and 1) for use as a radiation–detector by the following conclusions:

- All patterns show single phase with high stability of the crystalline structure and no other phases are found due to irradiation.
- The effect of irradiation is a compressive strain on the crystal lattice of samples which contain Zinc ion, but for the x=0.0 sample is elongation strain.
- The defect formed in the unit cell is due to the formation of ferrous ion.
- The calculation values are in good approaches with experimental values and they both have the same trend and it confirms the estimated cation distributions for NZGF samples.
- The effect of irradiation on the samples which contain Zn ions will increase the interaction cations at both sites (tetrahedral and octahedral), which increased the constant force and frequency band. And therefore, the irradiation by thermal neutrons of ferric ions changes to ferrous ions, this tends to shift of some absorbed bands.
- The magnetization parameters were decreased by introducing of Zn ions and by thermal neutron irradiation.

COMPETING INTERESTS

Author has declared that no competing interests exist.

REFERENCES

1. Chinnasamy CN, Narayanasamy A, Ponpandian N, Chattopadhyay K, Shinoda K, Jeyadevan B, Tohji K, Nakatsuka K. Mixed spinel structure in nanocrystalline $NiFe_2O_4$. Phys. Rev. B: Condens. Matter Mater. Phys. 2001;63: 184108–184114.

2. Carta D, Casula MF, Falqui A, Loche D, Mountjoy G, Sangregorio C, Corrias A. A structural and magnetic investigation of the inversion degree in ferrite nanocrystals MFe_2O_4 (M = Mn, Co, Ni). J. Phys. Chem. C. 2009;113:8606–8615.

3. Guigue Millot N, Begin-Colin S, Champion Y, H'tch M, Le Caer G, Perriat P. Control of grain size and morphologies of nanograined ferrites by adaptation of the synthesis route: Mechanosynthesis and soft chemistry. J. Solid State Chem. 2003;170:30–38.

4. Mouallem-Bahout M, Bertrand S, Pena O. Synthesis and characterization of $Zn_{1-x}Ni_xFe_2O_4$ spinels prepared by a citrate precursor. J. Solid State Chem. 2005;178: 1080–1086.

5. Jung CW, Jacobs P. Magn. Reson. Imaging, physical and chemical properties of superparamagnetic iron oxide mr contrast agents: Ferumoxides, ferumoxtran, ferumoxsil. 1995;13:661–674.

6. Ikenaga N, Ohgaito Y, Matsushima H, Suzuki T. Preparation of zinc ferrite in the presence of carbon material and its application to hot-gas cleaning Fuel. 2004; 83:661–669.

7. Imam NG, Hashhash A. Photoluminescence of γ-irradiation induced distortion on Ga based ferrospinel material to be used as γ-rays detector. Nuclear Instruments and Methods in Physics Research A. 2014;767:353–358.

8. Hassan HE, Sharshar T, Hessien MM, Hemed OM. Effect of γ-rays irradiation on Mn–Ni ferrites: Structure, magnetic properties and positron annihilation studies. Nuclear Instruments and Methods in Physics Research B. 2013;304:72–79.

9. Eltabey MM, Ali IA, Hassan HE, Comsan MNH. Effect of γ-rays irradiation on the structure and magnetic properties of Mg–Cu–Zn ferrites. J Mater Sci. 2011;46:2294–2299.

10. Jagadeesha Angadi V, Anupama AV, Harish K. Choudhary R, Kumar HM,

Somashekarappa M, Mallappa B, Rudraswamy B, Sahoo. Mechanism of γ-irradiation induced phase transformations in nanocrystalline Mn0.5Zn0.5Fe2O4 ceramics. Journal of Solid State Chemistry. 2017;246:119–124.

11. Elalaily NA, Mahamed RM. Effects of fast neutron and gamma irradiation on electrical conductivity of some borate glasses. Journal of Nuclear Materials. 2002;303:44–5.

12. Hashhash A, Yehia M, Ismail SM, Ata-Allah SS. Structural and magnetic study of Zn-substituted $NiGa_yFe_{2-y}O_4$ ferrite. J Supercond Nov Magn. 2014;27:2305–2310.

13. Ata-Allah SS, Balagurov AM, Hashhash A, Bobrikov IA, Hamdy Sh. Refinement of atomic and magnetic structures using neutron diffraction for synthesized bulk and nano-nickel zinc gallate ferrite. Physica B. 2016;481:118–123.

14. Smit J. Magnetic properties of materials, McGraw-Hill book company, New York. 1971;22-23.

15. Shannon RD. Revised effective ionic radii and systematic studies of interatomic distances in halides and chalcogenides. Acta Cryst. A. 1976;32:751-767.

16. Lakhani VK, Pathak TK, Vasoya NH, Modi KB. Structural parameters and X-ray debye temperature determination study on copper-ferrite-aluminates. Solid State Sci. 201;13:539.

17. Rathod V, Anupama AV, Vijaya Kumar R, Jali VM, Sahoo B. Correlated vibrations of the tetrahedral and octahedral complexes and splitting of the absorption bands in FTIR spectra of Li-Zn ferrites, Vibrational Spectroscopy. 2017;92:267–272.

18. Stoner EC, Wohlfarth EP. A mechanism of magnetic hysteresis in heterogeneous alloys, Philos. Trans. R. Soc. Lond. A 1948;240(826):599–642.

19. Parvatheeswara Rao B, Dhanalakshmi B, Ramesh S, Subba Rao PSV. Cation distribution of Ni-Zn-Mn ferrite nanoparticles. Journal of Magnetism and Magnetic Materials. 2018;456:444–450.

20. Hamada IM. X-ray diffraction and IR absorption in the system $Co_{0.6}Zn_{0.4}Mn_xFe_{2-x}O_4$ before and after γ-irradiation. Journal of Magnetism and Magnetic Materials. 2004;271:318–325.

21. Hemeda OM, El-Saadawy M. Effect of gamma irradiation on the structural properties and diffusion coefficient in Co–Zn ferrite. Journal of Magnetism and Magnetic Materials. 2003;256:63–68.

22. MA Ahamed, Samiha T. Bishay, Radwan FA. γ Irradiation effect on the polarization and resistance of Li-Co-Yb- ferrite. J. phys. Chem. Solids. 2002;63:279-286.

23. Waldron RD. Infrared spectra of ferrites. Phys. Rev. 1955;99:1727.

24. Evans BJ, Hafner S. Mössbauer resonance of Fe^{57} in oxidic spinels containing Cu and Fe. J. Phys. Chem. Solids. 1968;29:1573.

25. Gabal MA, Bayoumy W. Effect of composition on structural and magnetic properties of nanocrystalline $Ni_{0.8-x}Zn_{0.2}Mg_xFe_2O_4$ ferrite, Polyhedron. 2010; 29:2569–2573.

26. Anupama AV, Rathod V, Jali VM, Sahoo. Composition dependent elastic and thermal properties of Li-Zn Ferrites. Journal of Alloys and Compounds. 2017;728:1091-1100.

27. Neel I. Ann. Phys. 1948;3:137.

Peer-review history:
The peer review history for this paper can be accessed here:
http://www.sdiarticle3.com/review-history/50239